

Integrated Sensing and Communication Channel Modeling: A Survey

Zhiqing Wei, *Member, IEEE*, Jinzhu Jia, Yangyang Niu, *Student Member, IEEE*, Lin Wang, *Student Member, IEEE*, Huici Wu, *Member, IEEE*, Heng Yang, Zhiyong Feng, *Senior Member, IEEE*

Abstract—Integrated sensing and communication (ISAC) is expected to play a crucial role in the sixth-generation (6G) mobile communication systems, offering potential applications in the scenarios of intelligent transportation, smart factories, etc. The performance of radar sensing in ISAC systems is closely related to the characteristics of radar sensing and communication channels. Therefore, ISAC channel modeling serves as a fundamental cornerstone for evaluating and optimizing ISAC systems. This article provides a comprehensive survey on the ISAC channel modeling methods. Furthermore, the methods of target radar cross section (RCS) modeling and clutter RCS modeling are summarized. Finally, we discuss the future research trends related to ISAC channel modeling in various scenarios.

Index Terms—Integrated sensing and communication, 3rd Generation Partnership Project, radar sensing channel modeling, communication channel modeling, radar cross section, survey, review.

I. INTRODUCTION

Integrated sensing and communication (ISAC) provides the dual functions of radar sensing and communication in the same system, which is of great significance in the scenarios such as intelligent transportation, smart factories [1], [2], as shown in Fig. 1. ISAC achieves high-rate and low-latency communication, as well as high sensing accuracy by exploiting the mutual benefit between radar sensing and communication [3], [4]. The future mobile communication systems are characterized by high frequency bands, large bandwidth, and large antenna array, which are beneficial to sensing, enabling the implementation of ISAC technology.

The radar channel model reveals the characteristics of radar signal propagation, which is the cornerstone for signal processing, interference management, and performance evaluation of ISAC system [5]. In the 3rd Generation Partnership Project (3GPP) standards, random channels are usually applied to evaluate the performance of communication due to the low computational complexity. However, it lacks the modeling of the radar scattering cross sectional product of targets and environmental scatterers, which is essential for radar sensing. Fishler *et al.* [6] first proposed the concept of “radar channel”

considering the radar cross section (RCS) characteristic of target, which is mainly modeled by deterministic modeling methods [7] and statistical modeling methods [8]. The deterministic modeling methods have high computational complexity and limited application scenarios. Although the statistical modeling methods have a wide range of applications, they rely on a large amount of channel measurements.

The deterministic modeling methods utilize the principles of electromagnetic wave propagation to accurately predict the radar channel model. The accurate methods refer to solving the electromagnetic wave equation or the integral equation of the induction field distributed over the surface of target, including geometric optics (GO) [9], [10], physical optics (PO) [11], signal-based ray-tracing (SBR) [12], [13], etc. There have been some studies on the deterministic modeling of RCS. Adana *et al.* [14] proposed an RCS area calculation method for mono-static radar with complex targets based on the PO method and the stationary phase method (SPM). Zhang *et al.* [15] employed the ray-tracing method to predict radar signal propagation, achieving precise estimation of target RCS. As for statistical modeling methods, Swerling *et al.* [16], [17] proposed five statistical models for the fluctuation characteristic of targets in the 1960s, namely Swerling I to V models. In [18], several statistical models for the RCS of targets are introduced, including the chi-square model, the log-normal distribution model, and the Weibull model.

Moreover, clutter modeling also plays an essential role in radar channel modeling. Similar to the RCS modeling of target, the deterministic modeling and statistical modeling methods can be applied in clutter modeling. The RCS characteristics of clutter sources are closely related to the scenarios and the parameters of radar sensing. Deterministic modeling of clutter predicts the RCS characteristics of clutter cells. Taking the sea clutter as an example, the well-known deterministic models include the Georgia Institute of Technology (GIT) model [19], hybrid model [20], and Morchin model [21]. Furthermore, the clutter can be characterized by statistical modeling due to the random fluctuation of the amplitude of clutter. Drosopoulos *et al.* [22] verified that the sea clutter approximately follows the Gaussian distribution. The classical statistical models such as Marcum [23] and Swerling models [24] are applicable to low-resolution radars. However, the above-mentioned classical models fail to provide accurate predictions for the channel modeling of high-resolution radars [25]. Therefore, the log-normal, Weibull, and K -distribution models are proposed [26]. Nevertheless, it is difficult to accurately describe the characteristics of clutter using a single

Zhiqing Wei, Jinzhu Jia, Yangyang Niu, Lin Wang, Heng Yang and Zhiyong Feng are with Key Laboratory of Universal Wireless Communications, Ministry of Education, Beijing University of Posts and Telecommunications (BUPT), Beijing 100876, China (emails: weizhiqing@bupt.edu.cn, jiajinzhu@bupt.edu.cn, niuyy@bupt.edu.cn, wlwl@bupt.edu.cn, dailywu@bupt.edu.cn, yangheng@bupt.edu.cn, fengzy@bupt.edu.cn).

Huici Wu is with the National Engineering Lab for Mobile Network Technologies, Beijing University of Posts and Telecommunications (BUPT), Beijing 100876, China (e-mail: dailywu@bupt.edu.cn).

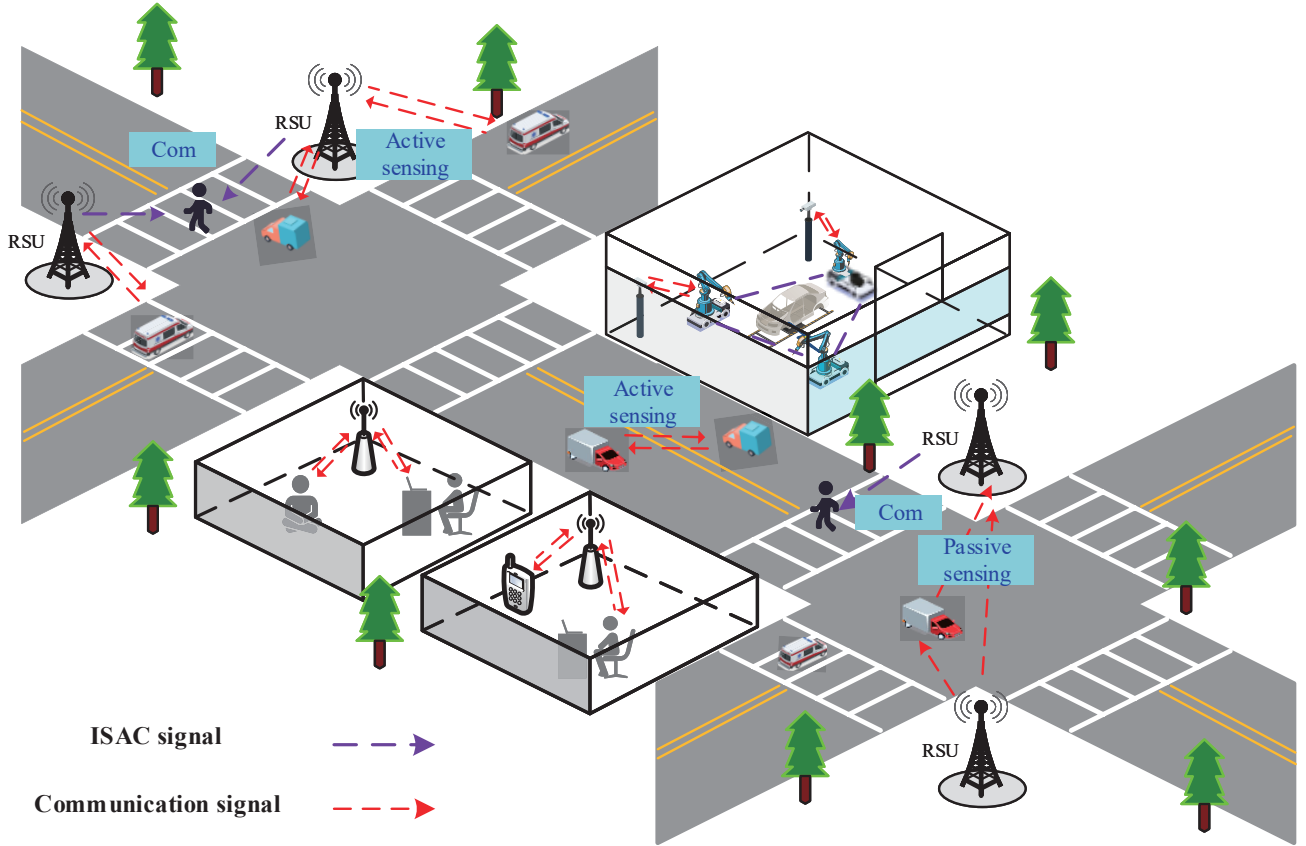


Fig. 1. Application scenarios of ISAC systems.

TABLE I: List of abbreviations

3GPP	3rd Generation Partnership Project	6G	Sixth-generation
BS	Base station	PDF	Probability density function
CDL	Clustered delay line	DoF	Degree of freedom
EM	Electromagnetic methods	FDTD	Finite-difference time-domain
FMM	Fast multipole method	GC-PDF	Generalized compound probability density function
GMDM	Gaussian mixture density model	GO	Geometric optics
ISAC	Integrated sensing and communication	LOP	Legendre orthogonal polynomials
LoS	Line-of-sight	MoM	Method of moment
NLoS	Non-line-of-sight	PO	Physical optics
RCS	Radar cross section	SBR	Signal-based ray-tracing
SPM	Stationary phase method	TDL	Tapped delay line
UE	User equipment	UTD	Uniform theory of diffraction

statistical model [27]. To accurately describe the temporal and spatial characteristics of clutter, the compound statistical modeling methods are proposed by adjusting the model parameters [28] [29].

The clustered delay line (CDL) and tapped delay line (TDL) channel models are used to model the communication channels such as the one-way channel between the transmitter and the receiver in 3GPP TR 38.901 [30]. However, in the ISAC systems, the transceiver detects the target through the received echo signal reflected from target. Thus, the radar channel needs to establish a round-trip channel model. The above-mentioned communication channels can be modified by introducing coefficients such as RCS to model the radar channel [31]. Hence, it is feasible to establish radar channel models based on the communication models, which provide references for radar channel modeling. Overall, the differences between communication channels and radar channels are summarized as follows.

- **Difference in the locations of transceiver:** The transmit communication data is inherently stochastic [32]. Consequently, the transmitter and receiver in communication system are spatially separated. The sensing signal is well-defined and structured to estimate the location, velocity, or image of target. Radar sensing modes consist of active sensing and passive sensing [33]. In active sensing, the transmitter and receiver are co-located, while they are separately located in passive sensing.
- **Difference in the application scenarios:** Communication systems perform channel estimation based on received communication signal [32]. Conversely, radar system estimates the distance, location, direction, and image of target using the received echo signal [33]. In communication system, multipaths are beneficial to spatial diversity. However, in radar system, active sensing relies on a line-of-sight (LoS) link for target detection and the parameters estimation, while a non-line-of-sight (NLoS) link will lead to false alarm [34].
- **Difference in channel fading:** Channel fading is mainly characterized by large-scale and small-scale fading in communication systems, modeling the propagation loss of communication signals over a transmission range. However, the fading coefficients are mainly related to the scattering characteristics of target in radar sensing channel, including target RCS and clutter RCS.

The deviation in random channel modeling methods will impact the sensing accuracy. In contrast, deterministic channel modeling methods accurately characterize radar channel. Li *et al.* proposed the GO, PO, and Electromagnetic method (EM) to model radar channel [35]. Jing *et al.* proposed a measurement-based statistical channel modeling approach, which is applied to scatter-based spatial channel models [36]. Overall, there are rich research achievements in the area of ISAC channel models. However, there are rarely survey articles summarizing ISAC channel modeling.

This article provides a comprehensive survey of the ISAC channel modeling. Specifically, the radar channel modeling and communication channel modeling methods are provided,

including the modeling of target RCS and clutter RCS from deterministic and statistical perspectives. The structure of this article is illustrated in Fig. 2. In Section II, we provide a brief overview of the channel modeling of ISAC in both active and passive sensing modes. Section III and IV provide the modeling methods for target RCS and clutter RCS, respectively. Section V summarizes the future research trends and Section VI concludes this article. The abbreviations used in this article are listed in Table I.

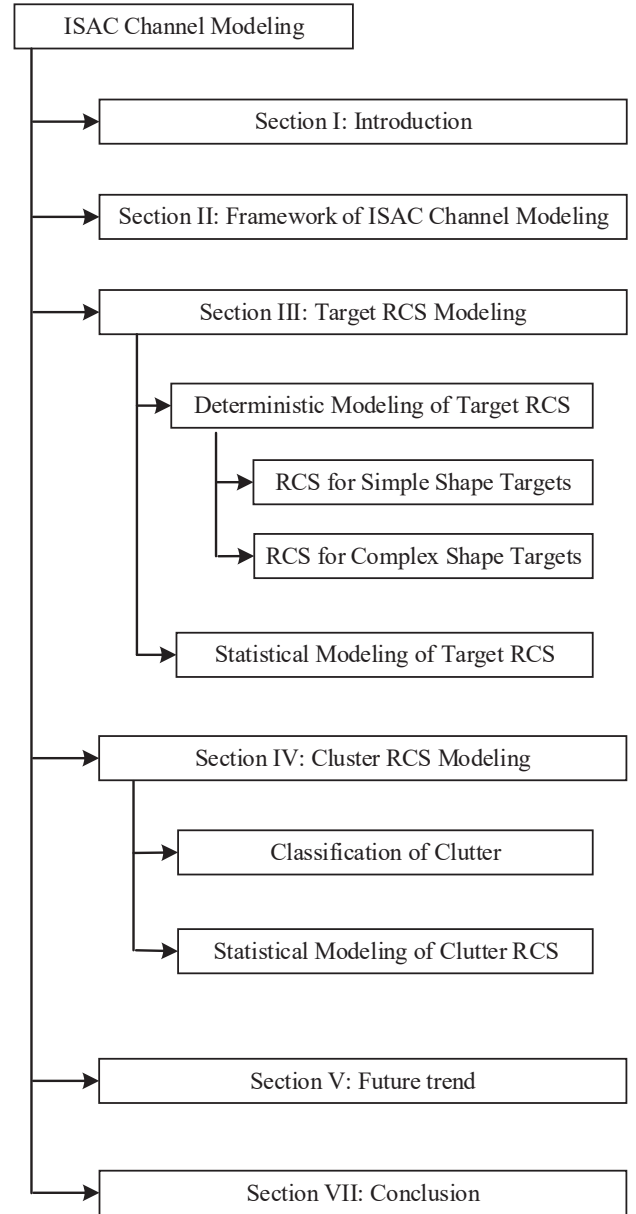


Fig. 2. The structure of this article.

II. FRAMEWORK OF ISAC CHANNEL MODELING

In this section, the framework of ISAC channel modeling is introduced. Specifically, The communication and radar sensing

channel modeling methods are reviewed for active and passive sensing, respectively.

A. Active Sensing

In active sensing mode, the transmitter and receiver are deployed in the same device. The active sensing device can be either the base station (BS) or the user equipment (UE). Take the BS as an example, the BS transmits ISAC signal to UE, while receiving the echo signal for target sensing, as shown in Fig. 3. The ISAC channel include the one-way communication channel following the path “BS→UE” and the two-way sensing channel following the path “BS→target→BS”.

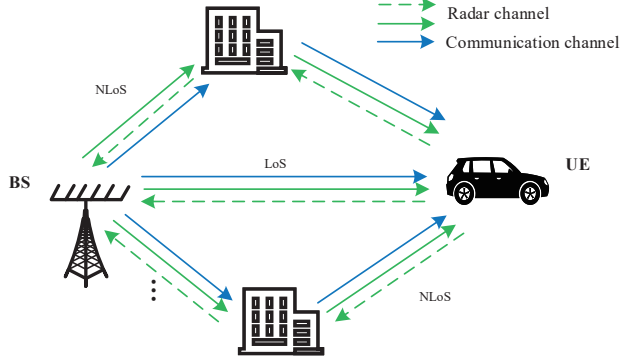


Fig. 3. ISAC channel of active sensing.

1) *One-way communication channel*: The one-way communication channel can be expressed as [31]

$$\mathbf{H}_{com}^{act} = \sqrt{N_t N_r} \underbrace{\tilde{\alpha}_0 \mathbf{A}_r(\theta_r^0) \mathbf{A}_t^H(\theta_t^0)}_{(a)} + \sqrt{N_t N_r} \sum_{l=1}^{L_{path}-1} \underbrace{\tilde{\alpha}_l \mathbf{A}_r(\theta_r^l) \mathbf{A}_t^H(\theta_t^l)}_{(b)}, \quad (1)$$

where (a) is the LoS path component and (b) is the multipath component; N_t and N_r are the numbers of the transmitting and receiving antenna array elements, respectively; $\tilde{\alpha}_l$ is the fading coefficient of the l -th propagation path; $\mathbf{A}_r(\theta_r^l)$ and $\mathbf{A}_t^H(\theta_t^l)$ are the steering vectors of the receiving and transmitting antenna arrays for the l -th propagation path, respectively; θ_t^l and θ_r^l are the angle of arrival and angle of departure related to the l -th propagation path, respectively; L_{path} is the number of propagation paths, and $l = 0$ represents the LoS path.

2) *Two-way sensing channel*: As shown in Fig. 3, the received echo signals reflected from the target experience a two-way sensing channel, which can be expressed as [31]

$$\mathbf{H}_{rad}^{act} = \sqrt{N_t N_r} \tilde{\alpha}_0 \tilde{\sigma}_0 \mathbf{A}_r(\theta_r^0) \mathbf{A}_t^H(\theta_t^0) + \sqrt{N_t N_r} \sum_{l=1}^{L_{path}-1} \tilde{\alpha}_l \tilde{\sigma}_l \mathbf{A}_r(\theta_r^l) \mathbf{A}_t^H(\theta_t^l), \quad (2)$$

where $\tilde{\sigma}_0$ is the RCS of target; $\tilde{\sigma}_l$ is the RCS of clutter generating by the scatter other than target, which are the key parameters in the two-way sensing channel. In addition, the

parameters $\mathbf{A}_r(\theta_r^l)$, $\mathbf{A}_t^H(\theta_t^l)$, $\mathbf{A}_r(\theta_r^l)$, $\mathbf{A}_t^H(\theta_t^l)$, θ_t^l , and θ_r^l have the same meaning to these parameters in (1).

B. Passive Sensing

As illustrated in Fig. 4, ISAC channel of passive sensing can be decomposed into the one-way communication channel and one-way sensing channel.

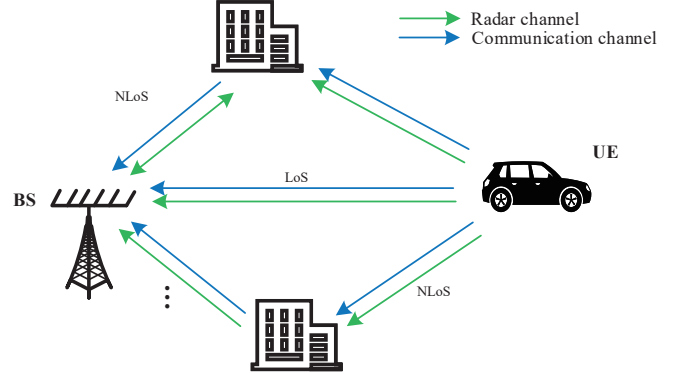


Fig. 4. ISAC channel of passive sensing.

1) *One-way communication channel*: The one-way communication channel model in passive sensing is the same to that in active sensing.

2) *One-way sensing channel*: As shown in Fig. 4, the radar signals in passive sensing experience one-way sensing channel from BS to UE. However, the radar sensing channel of passive sensing has the same form to that of active sensing in (2). According to (2), the radar sensing channel models are closely related with the RCS characteristics of target and scatter, which will be reviewed in Sections III and IV, respectively.

III. TARGET RCS MODELING

The RCS is employed to characterize the signal attenuation caused by target, influenced by the target’s geometric properties, surface material, and the wavelength of the incident electromagnetic wave [37], [38]. The modeling methods for target RCS can be categorized into deterministic modeling and statistical modeling methods, which will be reviewed in this section.

A. Deterministic Modeling of Target RCS

The deterministic modeling methods model the target RCS accurately and detailedly. Fig. 5 illustrates the classification of deterministic RCS modeling methods including geometry methods and numerical methods. Numerical methods calculate RCS accurately for the targets with complex shapes, which has high computational complexity and are better for small targets. In contrast, geometric methods provide fast calculation speed. However, they are only feasible for the target with size exceeding the wavelength.

TABLE II: RCS of objects with several simple geometric shapes [40]

Object	RCS	Observation Direction
Sphere (radius R)	πR^2	Any direction
Flat circular plate (radius a)	$\frac{4\pi^3 a^4}{\lambda^2}$	Parallel to the normal
Cylindrical (length L , radius a)	$\frac{2\pi a L^2}{\lambda}$	Perpendicular to the axis of symmetry
Flat plate (area A)	$4\pi \frac{A^2}{\lambda^2}$	Parallel to the normal
Ellipsoid (semi-long axis a , semi-short axis b)	$\frac{\pi b^2}{a^2}$	Parallel to the long or short axis
Cone	$\frac{1}{16\pi} \lambda^2 \tan^4 \theta$	Parallel to the axis of symmetry

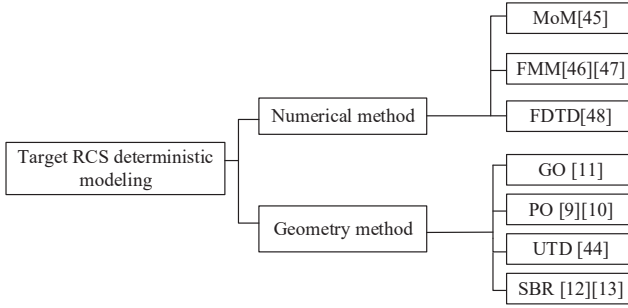


Fig. 5. Deterministic modeling methods of target RCS [39].

1) *RCS of the target with simple shape*: The RCS for the target with a simple geometric shape can be accurately obtained, especially for the point target, whose scattering property is isotropic, making the RCS independent of the angle of incidence. For instance, the RCS of a uniformly dense metal sphere with radius R can be straightforwardly calculated as πR^2 [41]. For complicated shapes such as uniform circular plates with radius R , the scattering properties are angle-dependent, leading to varying RCS in different incident angles, which can be expressed as [41]

$$\sigma_C = \frac{4\pi^3 R^4}{\lambda^2} \left[\frac{2J_1\left(\frac{4R \sin \psi}{\lambda}\right)}{\frac{4R \sin \psi}{\lambda}} \right] \cos^2 \psi, \quad (3)$$

where λ is the wavelength, ψ is the angle between the incidence ray and the plane's normal vector, and $J_1(\cdot)$ is the first-order Bessel function. The RCS of the target with different geometric shapes is listed in TABLE II [41].

2) *RCS of the target with complicated shape*: The above calculation methods of RCS are feasible for the target with a simple shape, as shown in TABLE II. In the practical scenario, a complicated target typically includes discrete components with complex geometries, making it challenging to establish accurate RCS models. Therefore, in the modeling methods for the RCS of the object with complex shape, the object is considered as a collection of simple scatterers. Due to the inflexibility and high computational complexity of the statistical averaging methods, various deterministic modeling methods are proposed to accurately model the RCS of complicated targets, such as PO method [9], [10], GO method [11], SBR

method [12], [13], MoM [42], graphical electromagnetic calculation [43], etc. Several representative deterministic modeling methods are summarized as follows.

- **PO method** [9], [10]: The PO method calculates the scattered field across the target by integrating the induced electric field on the surface of target to derive the target's RCS. This method relies on the following conditions: 1) the curvature radius of target's surface is larger than the wavelength; 2) the target satisfies the far-field condition, which necessitates detecting the target from a distance ten times greater than the wavelength. For example, in terms of millimeter-wave radar, the PO method can quickly and accurately analyze a target's scattered field as long as the distance between the target and the radar is greater than 10 cm. However, the PO method neglects the impact of the discontinuities of target surface on the induced current, which leads to the inaccuracy of the RCS calculation results.
- **GO method** [11]: The GO method involves dividing the echo signals from a target into illuminated regions and shadowed regions and then determines the scattering centers using Fermat's principle. In this method, the scattered field of the target is calculated as the summation of scattered fields reflected from all scattering centers, enabling the calculation of the target's RCS. This method has stringent requirements: 1) the target's size must be significantly larger than the incident wavelength; 2) the electromagnetic wave must be isotropic, therefore approximate to a plane wave. Radar energy propagation can be approximated by electromagnetic waves propagating in tubes. And the influence between each beam is small. However, the GO method does not consider the scattering effect caused by diffraction. When the target has no curvature or single curvature, the obtained RCS will be infinite.
- **Signal-based ray-tracing (SBR) method** [12], [13]: The SBR method involves emitting rays in various directions through the transmitter to study the reflection characteristics of the rays in space and then predicts all paths during the signal propagation process. Moreover, the theory of electromagnetic wave propagation is applied to calculate the received power and time delay spread of each ray to analyze the channel characteristics. The SBR method combines the advantages of PO method and GO method,

possessing high accuracy in RCS modeling. Therefore, it is widely adopted in direct modeling of RCS. However, the SBR method has high computational complexity [44].

- **Uniform theory of diffraction (UTD) method** [45]: The UTD method effectively combines the advantages of PO and GO methods. It divides the scattering into physical optical, geometric optical, and diffraction regions, allowing for separated RCS calculations in each region. UTD is particularly suitable for accurately estimating RCS for large and intricate targets, as it takes into account the factors such as multiple reflections and target diffractions. However, it is associated with high computational complexity and does not consider the impact of target surface roughness on RCS. As a result, it can not provide accurate RCS calculations for the scattering scenarios with close-range. Moreover, Weinmann proposed a hybrid GO-PO-UTD method to enhance the estimation accuracy of target RCS [45].
- **Method of moment (MoM)** [46]: The MoM method regards the radar signal as a vector consisting of the target scattering center and scattering intensity. Then, the matrix decomposition methods are utilized to find the RCS of target. The MoM method is suitable for the target with uniform scattering distribution and appropriate size, and is particularly effective in calculating the low-frequency scattering of target. Due to the robustness and noise resistance capability, the MoM method is preferred in practice. However, the MoM method has drawbacks such as prolonged computation times and sensitivity to parameter selection. To tackle these problems, an improved MoM method is introduced to enhance the accuracy of RCS [46].
- **Fast multipole method (FMM)** [47], [48]: The FMM method utilizes a hierarchical network architecture to decompose the target into small components. Then, a fast multi-pole algorithm is used to calculate the scattered field of target, thus obtaining the RCS of target [47]. The FMM method is effective in accurately determining the RCS for various targets. As the complexity of target increases, the computation time increases correspondingly. However, there is still an advantage over the MoM algorithm in terms of computational complexity [48].
- **Finite-difference time-domain (FDTD) method** [49]: The FDTD method calculates the RCS of target by discretizing in both space and time domains to solve Maxwell's equations, resulting in the spatio-temporal distribution of the electromagnetic field [49]. The FDTD method stands out in accurately computing the RCS of complex-shaped target by effectively simulating its reflection and scattering characteristics. However, the FDTD method also faces the challenges such as high computational complexity, intricate parameter selection, and specific medium property requirements. Therefore, practical applications demand parameter optimization and low complexity algorithm.

B. Statistical Modeling of Target RCS

In practical scenario, the moving target with constantly changing position and angle of view will lead to the fluctuations in their cross-sectional areas, requiring the application of statistical methods to model the RCS of target [61]. Statistical methods model the RCS within a resolution cell as a random variable with specific probability density function (PDF). The PDF describes the statistical properties of RCS, where it is assumed that the target consists of several independent scatterers at random positions. The RCS of each scatterer is independent and constant. The characteristics of different statistical models are provided in Table III and the details are summarized as follows.

1) *Swerling I-V models*: Swerling *et al.* [16], [17] introduced five Swerling models (i.e. Swerling I-V), which are appropriate for the scenarios with fast fluctuation, slow fluctuation, and no fluctuation [16], [17].

- **Swerling I model** is applicable for slow fluctuating target, whose RCS follows Rayleigh distribution.
- **Swerling II model** is applicable for fast fluctuating target, whose RCS follows Rayleigh distribution.
- **Swerling III model** is applicable for slow fluctuating target, whose RCS follows Rice distribution.
- **Swerling IV model** is applicable for fast fluctuating target, whose RCS follows Rice distribution.
- **Swerling V model** is applicable for non-fluctuating target, whose RCS is a constant.

In these models, a slowly moving target implies that the echo signals within the same scanning period are correlated, and uncorrelated for different scanning periods. For a fast-fluctuating target, the echo signals are independent between pulses in the same scan. The Swerling I-IV models only consider fast and slow fluctuations of the amplitude of echo signals, which could model a majority of the target RCS in practice.

The RCS of target is denoted by σ . Suppose that $\bar{\sigma}$ represents the average target fluctuation throughout the entire observation process. The PDFs of Swerling I and II models are the same, which are given by [16]

$$f(\sigma) = \frac{1}{\bar{\sigma}} \exp\left(-\frac{\sigma}{\bar{\sigma}}\right), \sigma \geq 0. \quad (4)$$

The PDFs of Swerling III and IV models are the same, given by

$$f(\sigma) = \frac{4\sigma}{\bar{\sigma}^2} \exp\left(-\frac{2\sigma}{\bar{\sigma}}\right), \sigma \geq 0. \quad (5)$$

2) *Chi-square distribution model* [50]–[52]: Supposing that the target consists of a strong scatterer and a group of weak scatterers, the RCS can be modeled by chi-square distribution, which is given by [52]

$$f(\sigma) = \frac{1}{2^{\frac{n}{2}} \Gamma(\frac{n}{2})} \sigma^{\frac{n}{2}-1} \exp\left(-\frac{\sigma}{2}\right), \sigma > 0, \quad (6)$$

where n is the degree of freedom (DoF). Fig. 6 shows the PDF of chi-square distribution with different n . The Swerling I-V models mentioned above correspond to chi-square distributions with DoF of 1, 2, N , $2N$ or infinity. The chi-square

TABLE III: Characteristics of different statistical models of RCS

Type	Parameters	Computational complexity	Accuracy	References
Swerling I	Single	Low	Low	[16], [17]
Swerling II	Single	Low	Low	[16], [17]
Swerling III	Double	Low	Low	[16], [17]
Swerling IV	Double	Low	Low	[16], [17]
Swerling V	Single	Low	Low	[16], [17]
Chi-square distribution	Double	Low	Low	[18], [50]–[52]
Weibull distribution	Double	Low	Low	[18], [53]
Log-normal distribution	Double	Low	Medium	[18], [50], [51], [54]
Rice distribution	Double	Medium	Low	[55]
GMDM	Semi	High	High	[56]–[58]
Lejeune polynomial	None	High	High	[50], [59], [60]

distribution model is more applicable when the detection target is a regularly shaped object.

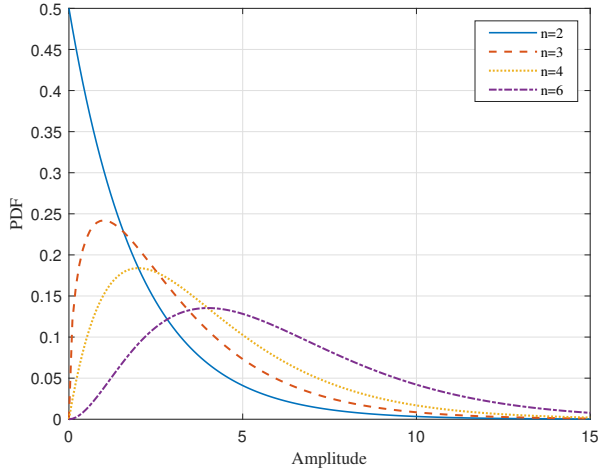


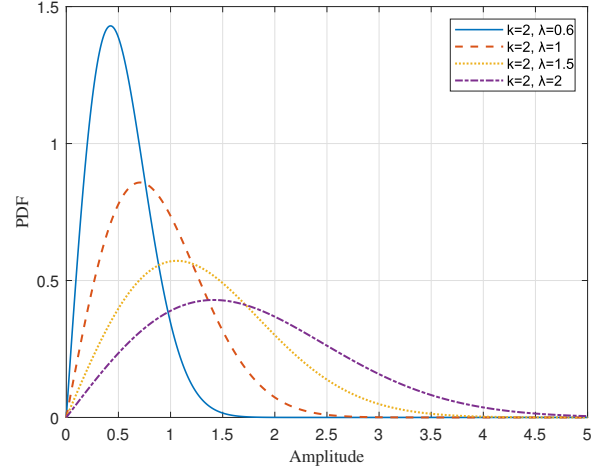
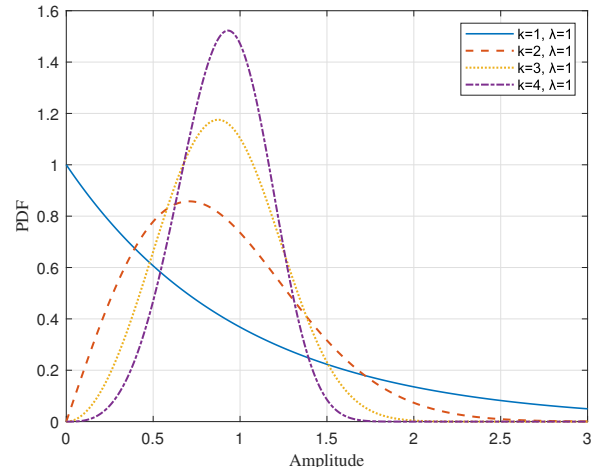
Fig. 6. The PDF of chi-square distribution.

3) *Weibull distribution model* [53]: The Weibull distribution is commonly utilized to model the RCS of moving target, which is given by [53]

$$f(\sigma; k, \lambda) = \frac{k}{\lambda} \left(\frac{\sigma}{\lambda}\right)^{k-1} \exp\left(-\frac{\sigma}{\lambda}\right), \sigma > 0, \lambda > 0, k > 0, \quad (7)$$

where k is the shape factor, λ is the scale factor. Fig. 7 shows the PDF of Weibull distribution with different λ and Fig. 8 shows the PDF of Weibull distribution with different k . It is worth mentioning that the Weibull model approximately fits the chi-square distribution when the shape and scale factors are known.

4) *Log-normal model* [50], [51]: Wang *et al.* [62] discovered that when the RCS distribution is a single-peaked distribution, the log-normal distribution model has higher accuracy

Fig. 7. The PDF of Weibull distribution with different λ .Fig. 8. The PDF of Weibull distribution with different k .

compared with the Weibull and chi-square distributions. The PDF of log-normal distribution can be expressed by [27]

$$f(\sigma; \mu, s) = \frac{1}{s\sigma\sqrt{2\pi}} \exp(-(\ln \sigma - \mu)^2), \sigma > 0, \quad (8)$$

where s is the standard deviation and μ is the variance. Fig. 9 and Fig. 10 show the PDF of log-normal distribution with different s and μ , respectively. It is observed that the mean affects the position of the curve, with an increase or decrease in the mean directly causing the center axis of the curve to move left or right. Beside, the variance influences the width and height of the curve, with an increase in variance causing the curve to become wider and the tails flatter. The log-normal distribution is effective for modeling the RCS of the target with large size and high velocity. However, its accuracy is diminishing with the increase of the target's velocity [54].

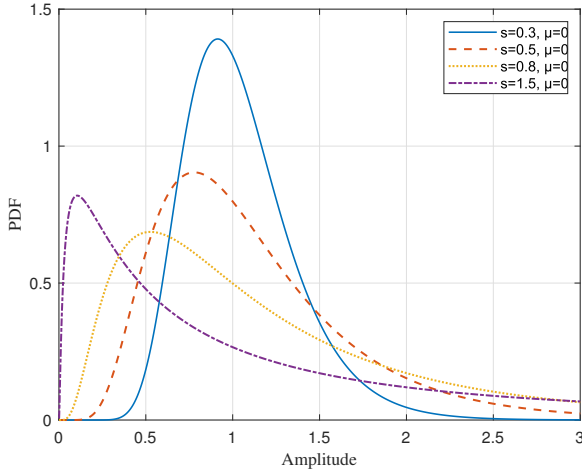


Fig. 9. The PDF of log-normal distribution with different s .

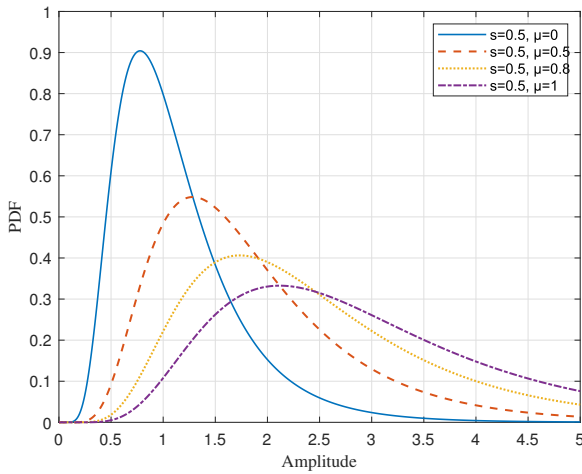


Fig. 10. The PDF of log-normal distribution with different μ .

5) *Rice distribution model* [55]: The PDF of the Rice distribution is [63]

$$f(\sigma; \lambda, k) = \frac{1}{k} \exp\{-\lambda - \frac{\sigma}{k}\} I_0(2\sqrt{\frac{\lambda\sigma}{k}}), \sigma > 0, \quad (9)$$

where $I_0(\cdot)$ is the 0-order Bessel function, λ is the scale factor, and k is the shape factor. Fig. 11 and Fig. 12 show the PDF of Rice distribution with different λ and k , respectively. Moreover, the Rice distribution is similar to the chi-square distribution, particularly in the case that the values of λ and k are approximately equal. However, in practical scenarios, the RCS of target is dynamic, and the Rice distribution model demonstrates poor performance due to the diverse factors influencing target characteristics.

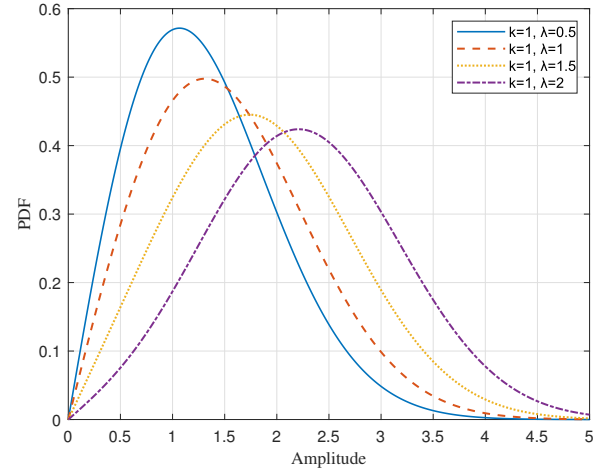


Fig. 11. The PDF of Rice distribution with different λ .

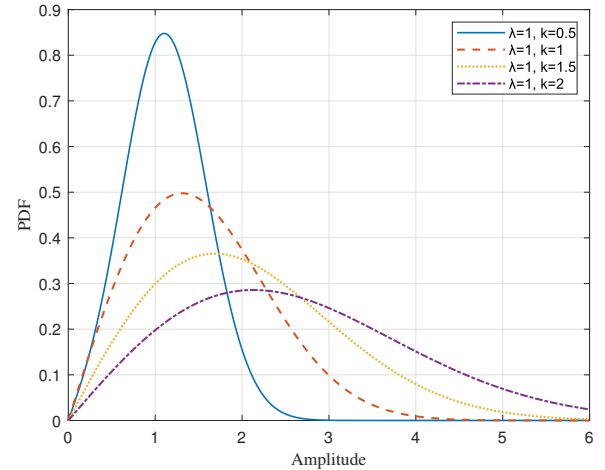


Fig. 12. The PDF of Rice distribution with different k .

6) *Gaussian mixture density mode (GMDM)* [56]–[58]: When the movement and trajectory of target are changing, the above RCS statistical models are no longer available [64]. Zhuang *et al.* [65] proposed a Gaussian mixture density mode (GMDM)-based statistical model to describe the RCS of the target with time-varying mobility. GMDM is a semi-parametric model that utilizes a mixture of multiple Gaussian distributions. Then, the PDF of the M -order GMDM can be

expressed as [56], [57]

$$f(\sigma; Q) = \sum_{i=1}^M \frac{a_i}{\sqrt{2\pi\sigma_i^2}} \exp\left(-\frac{(\sigma - \mu_i)^2}{2\sigma_i^2}\right), \quad (10)$$

where μ_i and σ_i^2 are the mean and variance of the i -th Gaussian distribution, respectively, a_i satisfies $\sum_{i=1}^M a_i = 1$, and Q denotes $\{a_1, a_2, \dots, a_M; \mu_1, \mu_2, \dots, \mu_M; \sigma_1^2, \sigma_2^2, \dots, \sigma_M^2\}$. Zhuang *et al.* [58] applied the GMDM to model the dynamic RCS of aircraft, whose accuracy improves with the increase of M . However, it concurrently results in high complexity.

7) *Legendre orthogonal polynomials (LOP) Model* [50], [59], [60]: The parametric model establishes a certain PDF with finite parameters. In contrast, non-parametric model is more flexible than parametric model. In order to obtain accurate RCS model of the target with high mobility, the non-parametric model of RCS is widely studied. In particular, LOP model is a common non-parametric model, which requires a combination of central moments and LOP to approximate the PDF of the non-parametric model [59]. Hence, it is only necessary to calculate the central moments of all N -th order observed values and the LOP will fit the RCS with arbitrary accuracy. Then, the PDF of LOP model is given by [60]

$$f(\sigma) = \frac{1}{\sigma_L} f\left(\frac{\sigma - \bar{\sigma}}{\sigma_L}\right) = \frac{1}{\sigma_L} \sum_{i=0}^{\infty} a_i L_i\left(\frac{\sigma - \bar{\sigma}}{\sigma_L}\right), \quad (11)$$

where σ_L is the interval length, i.e. $\sigma_L = \sigma_{\max} - \sigma_{\min}$, $L_i(\cdot)$ is Legendre polynomial, and a_i is determined by the k -th central moment of σ . The RCS fitting accuracy is improving when the order N is increased from 15 to 25. The non-parametric model fits well in practice with the cost of high complexity. Implementing the Lejeune polynomial model still lacks fast algorithms.

IV. CLUTTER RCS MODELING

Radar clutter refers to the scattered echoes caused by the objects other than the target, characterized by clutter RCS [66]. Clutter RCS is influenced by wavelength, polarization, and angle of incidence. The clutter RCS is a crucial performance metric describing the scattering cross-sectional area of clutter, offering valuable insights into the performance analysis and signal processing in radar sensing. This section introduces the classification of clutter, followed by an in-depth exploration on the various statistical models of clutter RCS.

A. Classification of Clutter

According to the application scenarios, clutter is categorized into three types, namely sea clutter, ground clutter, and meteorological clutter [37], [67]. Sea clutter is the scattered echoes produced by incident electromagnetic waves passing over the sea surface [68]. The scattering coefficient of sea clutter is related to the wind speed, wind direction, angle of incidence, and the state of sea surface [69]–[71]. Ground clutter is defined as the extraneous echoes received by radar when detecting the target on ground. Ground clutter is impacted by the angle of incidence, the ground's physical characteristics, and the

coverage area of radar beam [72]. Meteorological clutter is the scattered echoes when a radar signal passes through clouds, rain, snow, hail, etc. Meteorological clutter is mainly related to the state of air and the coverage volume of radar beam.

B. Statistical Modeling of Clutter RCS

Radar clutter is the sum of numerous echoes reflected from scatterers within the coverage of radar. The scatterers will cause variations of echoes, resulting in random fluctuations in clutter RCS [73], [74]. The RCS characteristic of clutter is usually described by the PDF of clutter. Moreover, the commonly used statistical models including Rayleigh distribution [75], log-normal distribution [76], [77], Weibull distribution [78], and K -distribution [79], [80]. Table IV summarizes the characteristics of statistical models of clutter RCS. The details of these distributions are introduced as follows.

1) *Rayleigh distribution clutter model*: Supposing that the clutter RCS is σ_C and the variance is k^2 , the PDF of the Rayleigh distribution clutter model is given by [91]

$$f(\sigma_C) = \frac{2\sigma_C}{k^2} \exp\left(-\frac{\sigma_C^2}{k^2}\right). \quad (12)$$

When the clutter cell consists of several independent weak scatterers, the RCS of clutter can be modeled by Rayleigh distribution, which is suitable for describing meteorological clutter and ground clutter. Fig. 13 shows the PDF of Rayleigh distribution with different variances. It can be observed that when k^2 equals 1, the Rayleigh distribution is equivalent to the chi-square distribution with 2 degrees of freedom. As the k^2 increases, the PDF curve becomes flatter.

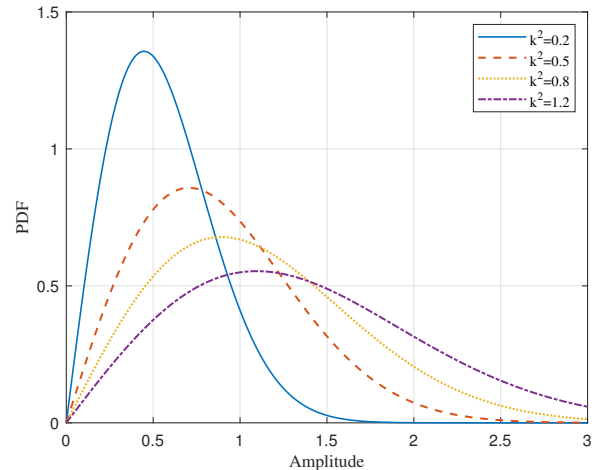


Fig. 13. The PDF of Rayleigh distribution with different k^2 .

2) *Log-normal distribution clutter model*: The PDF of log-normal distribution can be expressed as [50]

$$f(\sigma_C; \mu, s) = \frac{1}{s\sigma_C\sqrt{2\pi}} \exp\left(-\frac{(\ln \sigma_C - \mu)^2}{s^2}\right), \sigma > 0, \quad (13)$$

where $\ln \sigma_C$ follows normal distribution with standard deviation s and variance μ . The log-normal distribution is suitable for modeling the RCS of the ground clutter with small incidence angles and simple topography, and sea surface

TABLE IV: Characteristics of statistical models of clutter RCS

Category	Parameter	computational complexity	Accuracy	References
Rayleigh Distribution	Double	Low	Low	[75]
Log-normal distribution	Double	Low	Medium	[81], [82]
Weibull distribution	Double	Low	Medium	[78], [83], [84]
K -distribution	Double	Medium	High	[75], [82]
Generalized composite clutter model	Three	High	High	[85]–[90]

clutter with high-resolution requirements for radar systems. The shape parameter of log-normal distribution usually takes values between 0.5 and 1.3 [92]. Fig. 9 and Fig. 10 show the PDFs of log-normal distribution with different s and μ , respectively. It is revealed that when the μ is unchanged, the larger the s , the smaller the PDF peak and the longer its tail.

3) *Weibull distribution clutter model* : The PDF of the Weibull distribution model is [93]

$$f(\sigma_C; k, \lambda) = \frac{k}{\lambda} \left(\frac{\sigma_C}{\lambda}\right)^{k-1} \exp\left(-\frac{k}{\lambda}\right), \sigma_C > 0, \lambda > 0, k > 0, \quad (14)$$

where k is the shape factor, and λ is the scale factor. Fig. 7 and Fig. 8 show the PDF of the Weibull distribution with different λ and k , respectively. Note that when the shape parameter $k = 2$, the Weibull distribution is equivalent to the Rayleigh distribution, characterized by its heavy tail. It is commonly applied in the scenarios with high-resolution radar systems and shallow incidence angles [94].

4) *K -distribution clutter model*: The PDF of K -distribution model can be expressed as [95]

$$f(\sigma_C; k, \lambda) = \frac{2}{k\Gamma(\lambda+1)} \left(\frac{\sigma_C}{2k}\right)^{\lambda+1} I_{\lambda}\left(\frac{\sigma_C}{k}\right), \sigma_C > 0, \lambda > -1, \quad (15)$$

where k is the shape factor, λ is the scale factor, $I_{\lambda}(\cdot)$ is the λ -order modified Bessel function of the first kind and $\Gamma(\cdot)$ is the gamma function. The K -distribution is widely applied in modeling ground and sea clutter with high-resolution radar systems and shallow incidence angles [96]. Rayleigh, log-normal, and Weibull distributions are all derived from single-point statistics, lacking the ability to model the temporal and spatial correlations of clutter. In contrast, the K -distribution effectively models the spatio-temporal characteristics of clutter.

Figs. 14 and 15 show the PDFs of K -distribution with different λ and different k , respectively. The k parameter significantly influences the tail shape of the PDF, with an increase in k extending the tail. Conversely, the λ parameter correlates solely with the mean value of the clutter RCS. A smaller λ results in an extended tail, whereas as λ approaches infinity, the k -distribution converges towards a Rayleigh distribution. However, the accuracy of K -distribution is low for high-resolution radar systems. To improve the accuracy of K -distribution, KK -distribution is proposed to accurately simulate complex scattering effects in high-resolution radar

systems by establishing a hybrid model of two K -distributions in a high-resolution radar system [97].

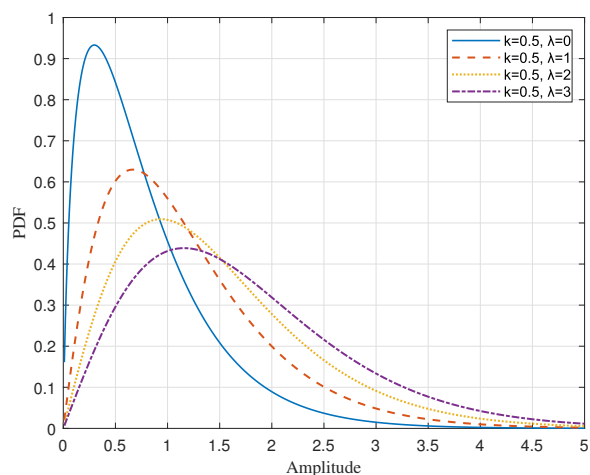


Fig. 14. The PDF of K -distribution with different λ .

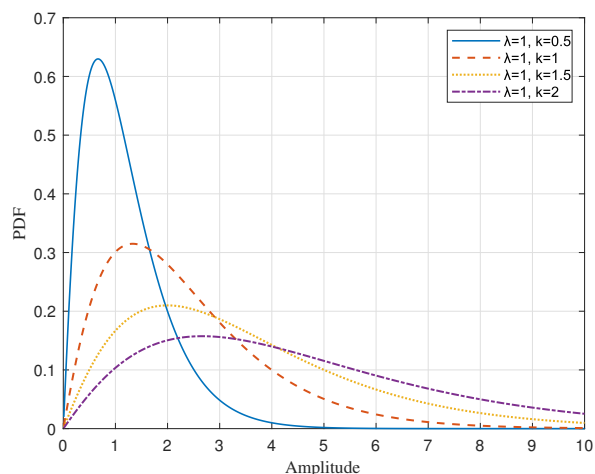


Fig. 15. The PDF of K -distribution with different k .

5) *Clutter composite statistical model*: With the increase in the frequency and resolution of radar systems, the K -distribution model does not satisfy the requirement of the modeling of the majority of clutters. Meanwhile, the composite K -distribution model describes the clutter amplitude as the

product of two factors, namely the speckle component and the amplitude modulation component. In this case, the speckle component, i.e., the fast-changing component, is formed by the superposition of the reflected phases of a large number of scatterers following Rayleigh distribution.

In high-resolution radar systems, a resolution cell typically contains a limited number of scatterers. The clutter exhibits non-Rayleigh characteristics due to the absence of phase references from numerous scatterers. Li *et al.* [98] introduced a generalized composite clutter RCS model with high flexibility, which is especially valuable in high-resolution radar systems. The PDF of the composite statistical model can be expressed as [99]

$$f(\sigma_C; k, \lambda) = \frac{|b|}{\lambda \Gamma(k)} \left(\frac{\sigma_C}{\lambda}\right)^{bk-1} \exp\left(-\left(\frac{\sigma_C}{\lambda}\right)^b\right), \lambda > 0, k > 0, \quad (16)$$

where k is the shape parameter, λ is the scale parameter, b is the power parameter of the Generalized Compound Probability Density Function (GC-PDF). This model is based on the premise that both the fast and slow variation components follow the generalized Gamma distribution. This clutter model is the exponential distribution when $b = 1$ and $\sigma_C = 1$. If $b = 2$, $\sigma_C = \frac{1}{2}$, and $\lambda = \sigma\sqrt{2}$, the clutter follows Gaussian distribution. If $b = 2$ and $\sigma_C = 1$, the clutter follows Rayleigh distribution. If $\sigma_C = 1$, the clutter follows Weibull distribution. Therefore, the exponential distribution, Gaussian distribution, Rayleigh distribution, and Weibull distribution are the special cases of the composite statistical model.

V. FUTURE TRENDS

This section provides the future research trends of ISAC channel modeling in the era of 6G, including ISAC channel measurement, ISAC channels for new applications, and ISAC channel models for cooperative sensing.

A. ISAC Channel Measurement

Efficient ISAC channel modeling is critical for the performance evaluation of ISAC system. Recently, the propagation characteristics of radar sensing channels are measured [100]. The relation between the radar sensing channel and parameters such as distance and angle in an ideal open-field scenario is investigated. However, the impact of non-ideal environment on channel modeling is rarely considered. In non-ideal environment, [101] and [102] have studied the relation between environmental parameters and ISAC channel characteristics. In indoor environment involving the sensing of human activities, [103] studied the impact of wall interference on ISAC channels. However, they mainly focused on the simple scatterer distribution. Wang *et al.* [104] explored the relation between environmental interference and radar sensing channels. To model the radar sensing channel, the traditional parameters not measured in communication channel measurement need to be measured. Zhang *et al.* [105] developed an ISAC channel measurement platform to analyze the channel characteristics of RCS, environmental information, and scatterer space information, laying a foundation for the study of ISAC channel modeling.

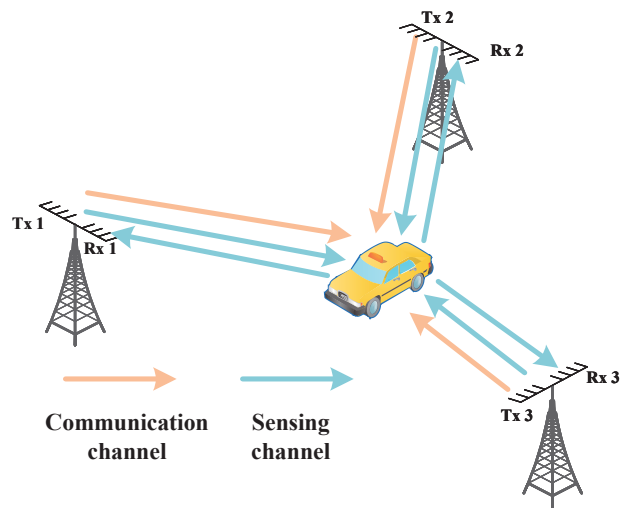


Fig. 16. The scenario of cooperative sensing.

B. ISAC Channel Models for New Applications

The complex electromagnetic propagation environment in the new applications of ISAC brings challenge for ISAC channel modeling. In this section, we investigate the ISAC channel modeling in the new applications including passive sensing for target localization and tracking, environmental reconstruction and target imaging, and gesture recognition.

1) *Passive sensing for target localization and tracking:* In target localization and tracking, the distance and velocity estimation are crucial. The target is commonly modeled as point by neglecting the volume and shape. In this application, ISAC channel modeling emphasizes the RCS characteristics of the point target [106]–[108].

2) *Environmental reconstruction and target imaging:* In this application, the accurate reconstruction of the positions of static, quasi-static, and dynamic scatterers in the surrounding environment is required. Meanwhile, specific scattering characteristics of these scatterers need to be modeled. In this application, ISAC channel modeling needs to consider various surface materials and features of scatterers [109].

3) *Gesture recognition:* In gesture recognition, the analysis of micro-Doppler information on moving targets is critical. In this application, ISAC channel modeling requires detailed parameters of gestures to ensure accurate recognition of gesture [110].

C. ISAC Channel Model for Cooperative Sensing

Recently, the cooperative sensing in ISAC system has attracted significant attention to break through the limitation of single-node sensing [111], [112], as shown in Fig. 16. Cooperative sensing fuses the sensing information of multiple nodes to realize accurate and large-scale sensing. Considering multiple nodes simultaneously detecting targets in cooperative sensing, the antenna arrays of multiple nodes can be viewed as a virtual antenna array and an equivalent radar sensing channel can be established based on the correlation between BSs [113]–[115].

VI. CONCLUSION

This article provides a comprehensive survey on ISAC channel modeling. Firstly, the channel modeling methods of ISAC channels with active and passive sensing modes are reviewed. Furthermore, the channel modeling methods for target RCS and clutter RCS are reviewed from both deterministic and statistical modeling perspectives. Finally, the future trends of ISAC channel modeling methods toward emerging applications in the 6G era are summarized. This article provides a guideline for channel modeling in ISAC systems.

REFERENCES

- [1] Y. Cui, F. Liu, X. Jing, and J. Mu, "Integrating sensing and communications for ubiquitous IoT: Applications, trends, and challenges," *IEEE Network*, vol. 35, no. 5, pp. 158–167, 2021.
- [2] Z. Wei, Y. Du, Q. Zhang, W. Jiang, Y. Cui, Z. Meng, H. Wu, and Z. Feng, "Integrated sensing and communication driven digital twin for intelligent machine network," *arXiv preprint arXiv:2402.05390*, 2024.
- [3] Z. Feng, Z. Fang, Z. Wei, X. Chen, Z. Quan, and D. Ji, "Joint radar and communication: A survey," *China Commun.*, vol. 17, no. 1, pp. 1–27, 2020.
- [4] A. Liu, Z. Huang, M. Li, Y. Wan, W. Li, T. X. Han, C. Liu, R. Du, D. K. P. Tan, J. Lu *et al.*, "A survey on fundamental limits of integrated sensing and communication," *IEEE Commun. Surv. Tutorials*, vol. 24, no. 2, pp. 994–1034, 2022.
- [5] W. Jiang, Z. Wei, Z. Feng, and X. Chen, "Integrated sensing and communication enabled sensing base station: System design, beamforming, interference cancellation and performance analysis," *arXiv preprint arXiv:2310.08263*, 2023.
- [6] E. Fishler, A. Haimovich, R. Blum, D. Chizhik, L. Cimini, and R. Valenzuela, "MIMO radar: An idea whose time has come," in *Proceedings of the 2004 IEEE Radar Conference (IEEE Cat. No. 04CH37509)*. IEEE, 2004, pp. 71–78.
- [7] S. M. Herman, "Joint passive radar tracking and target classification using radar cross section," in *Signal and Data Processing of Small Targets 2003*, vol. 5204. SPIE, 2004, pp. 402–417.
- [8] W. W. Weinstock, *Target cross section models for radar systems analysis*. University of Pennsylvania, 1964.
- [9] F. Chatzigeorgiadis, "Development of code for a physical optics radar cross section prediction and analysis application," NAVAL POST-GRADUATE SCHOOL MONTEREY CA, Tech. Rep., 2004.
- [10] J. Perez and M. Catedra, "Application of physical optics to the RCS computation of bodies modeled with NURBS surfaces," *IEEE Trans. Antennas Propag.*, vol. 42, no. 10, pp. 1404–1411, 1994.
- [11] C. Uluisik, G. Cakir, M. Cakir, and L. Sevgi, "Radar cross section (RCS) modeling and simulation, part 1: a tutorial review of definitions, strategies, and canonical examples," *IEEE Antennas Propag. Mag.*, vol. 50, no. 1, pp. 115–126, 2008.
- [12] Y. B. Tao, H. Lin, and H. Bao, "KD-tree based fast ray tracing for RCS prediction," *Progress In Electromagnetics Research*, vol. 81, pp. 329–341, 2008.
- [13] Y. Bennani, F. Comblet, and A. Khenchaf, "RCS of complex targets: original representation validated by measurements—application to ISAR imagery," *IEEE Trans. Geosci. Remote Sens.*, vol. 50, no. 10, pp. 3882–3891, 2012.
- [14] F. de Adana, I. Diego, O. Blanco, P. Lozano, and M. Catedra, "Method based on physical optics for the computation of the radar cross section including diffraction and double effects of metallic and absorbing bodies modeled with parametric surfaces," *IEEE Trans. Antennas Propag.*, vol. 52, no. 12, pp. 3295–3303, 2004.
- [15] J. A. Zhang, X. Huang, Y. J. Guo, J. Yuan, and R. W. Heath, "Multibeam for joint communication and radar sensing using steerable analog antenna arrays," *IEEE Trans. Veh. Technol.*, vol. 68, no. 1, pp. 671–685, 2018.
- [16] P. Swerling, "Radar probability of detection for some additional fluctuating target cases," *IEEE Trans. Aerosp. Electron. Syst.*, vol. 33, no. 2, pp. 698–709, 1997.
- [17] P. Swerling, "Recent developments in target models for radar detection analysis," in *AGARD Avionics Tech. Symp. Proc.*, 1970.
- [18] D. P. Meyer and H. A. Mayer, "Radar target detection- handbook of theory and practice," *New York, Academic Press, Inc.*, 1973. 508 p, 1973.
- [19] R. Paulus, "Evaporation duct effects on sea clutter," *IEEE Trans. Antennas Propag.*, vol. 38, no. 11, pp. 1765–1771, 1990.
- [20] G. Dockery, "Method for modelling sea surface clutter in complicated propagation environments," in *IEE Proceedings F (Radar and Signal Processing)*, vol. 137, no. 2. IET, 1990, pp. 73–79.
- [21] L. C. Rountree, "The radar range equation for the detection of steady targets in weibull clutter," AIR FORCE INST OF TECH WRIGHT-PATTERSONAFB OH, Tech. Rep., 1990.
- [22] A. Drosopoulos, "Description of the OHGR database." Defence Research Establishment Ottawa (Ontario), Tech. Rep., 1994.
- [23] J. Marcum, "A statistical theory of target detection by pulsed radar," *IRE Transactions on Information Theory*, vol. 6, no. 2, pp. 59–267, 1960.
- [24] P. Swerling, "Probability of detection for fluctuating targets," *IRE Transactions on Information theory*, vol. 6, no. 2, pp. 269–308, 1960.
- [25] K. Gerlach, "Spatially distributed target detection in non-gaussian clutter," *IEEE Trans. Aerosp. Electron. Syst.*, vol. 35, no. 3, pp. 926–934, 1999.
- [26] S. F. George, "The detection of nonfluctuating targets in log-normal clutter," NAVAL RESEARCH LAB WASHINGTON DC, Tech. Rep., 1968.
- [27] K. Ward and S. Watts, "Use of sea clutter models in radar design and development," *IET Radar Sonar Navig.*, vol. 4, no. 2, pp. 146–157, 2010.
- [28] D. Middleton, "New physical-statistical methods and models for clutter and reverberation: The KA-distribution and related probability structures," *IEEE J. Oceanic Eng.*, vol. 24, no. 3, pp. 261–284, 1999.
- [29] Y. Dong, "Distribution of X-band high resolution and high grazing angle sea clutter," DEFENCE SCIENCE AND TECHNOLOGY ORGANISATION EDINBURGH (AUSTRALIA) ELECTRONIC . . . , Tech. Rep., 2006.
- [30] 3GPP, "Study on enhancement of 3GPP support for 5G V2X services," *Tech. Rep. 22.886 V16. 2.0*, 2018.
- [31] X. Chen, Z. Feng, Z. Wei, P. Zhang, and X. Yuan, "Code-division OFDM joint communication and sensing system for 6G machine-type communication," *IEEE Internet Things J.*, vol. 8, no. 15, pp. 12093–12105, 2021.
- [32] K. Q. Zhang, *Wireless communications: principles, theory and methodology*. John Wiley & Sons, 2015.
- [33] P. Swerling, "Studies of target detection by pulsed radar," *IEEE Trans. Inf. Theory IEEE*, 1960.
- [34] D. Wright, J. Davies, T. Robinson, P. Chapman, T. Yeoman, E. Thomas, M. Lester, S. Cowley, A. Stocker, R. Horne *et al.*, "Space plasma exploration by active radar (SPEAR): an overview of a future radar facility," in *Annales Geophysicae*, vol. 18. Springer, 2000, pp. 1248–1255.
- [35] X. Li, J. He, Z. Yu, G. Wang, and P. Zhu, "Integrated sensing and communication in 6G: the deterministic channel models for THz imaging," in *2021 IEEE 32nd Annual International Symposium on Personal, Indoor and Mobile Radio Communications (PIMRC)*. IEEE, 2021, pp. 1–6.
- [36] G. Jing, J. Hong, X. Yin, J. Rodríguez-Piñeiro, and Z. Yu, "Measurement-based 3D channel modeling with cluster-of-scatterers estimated under spherical-wave assumption," *IEEE Trans. Wireless Commun.*, 2023.
- [37] N. Levanon, "Radar principles," *New York*, 1988.
- [38] D. K. Cheng *et al.*, *Field and wave electromagnetics*. Pearson Education India, 1989.
- [39] D. L. Herda, J. Suryana, and A. Izzuddin, "Radar cross section of F35: simulation and measurement," in *2020 6th International Conference on Wireless and Telematics (ICWT)*. IEEE, 2020, pp. 1–6.
- [40] B. R. Mahafza, *Radar systems analysis and design using MATLAB*. Chapman and Hall/CRC, 2005.
- [41] B. R. Mahafza, *Radar systems analysis and design using MATLAB*. USA: Chapman & Hall/CRC Press, Inc., 2022.
- [42] F. Weinmann, "Ray tracing with PO/PTD for RCS modeling of large complex objects," *IEEE Trans. Antennas Propag.*, vol. 54, no. 6, pp. 1797–1806, 2006.
- [43] J. M. Rius, M. Ferrando, and L. Jofre, "High-frequency RCS of complex radar targets in real-time," *IEEE Trans. Antennas Propag.*, vol. 41, no. 9, pp. 1308–1319, 1993.
- [44] J. Smit, J. Cilliers, and E. Burger, "Comparison of MLFMM, PO and SBR for RCS investigations in radar applications," 2012.
- [45] "UTD shooting-and-bouncing extension to a ."
- [46] M. Perotoni and S. Barbin, "A study on RCS of missile models using the method of moments," in *2007 SBMO/IEEE MTT-S International*

- Microwave and Optoelectronics Conference.* IEEE, 2007, pp. 492–495.
- [47] R. Coifman, V. Rokhlin, and S. Wandzura, “The fast multipole method for the wave equation: A pedestrian prescription,” *IEEE Antennas Propag. Mag.*, vol. 35, no. 3, pp. 7–12, 1993.
- [48] W. Nie and Z. Wang, “A hybrid approach for rapid computation of monostatic radar cross section problems with characteristic basis function method and singular value decomposition,” *The Applied Computational Electromagnetics Society Journal (ACES)*, pp. 844–850, 2019.
- [49] C. Moss, F. L. Teixeira, Y. E. Yang, and J. A. Kong, “Finite-difference time-domain simulation of scattering from objects in continuous random media,” *IEEE Trans. Geosci. Remote Sens.*, vol. 40, no. 1, pp. 178–186, 2002.
- [50] X. Xu and P. Huang, “A new RCS statistical model of radar targets,” *IEEE Trans. Aerosp. Electron. Syst.*, vol. 33, no. 2, pp. 710–714, 1997.
- [51] J. Follin Jr, F. Paddison, and A. Maffett, “Statistics of radar cross section scintillations,” *Electromagnetics*, vol. 4, no. 2-3, pp. 139–164, 1984.
- [52] M. Hejduk, “Improved radar cross-section “target typing” for spacecraft,” *Advances in the Astronautical Sciences*, vol. 135, no. 1, pp. 3–17, 2009.
- [53] E. J. Hughes, “Piecewise cumulative weibull modelling of radar cross section,” 2017.
- [54] Z. Q. Liu, L. J. Liang, Q. Y. Hu, C. Y. Wang, and J. S. Yang, “Influence on aircraft dynamic RCS statistical characteristics from flight speed,” in *2017 International Applied Computational Electromagnetics Society Symposium (ACES)*. IEEE, 2017, pp. 1–2.
- [55] D. Schiavulli, F. Nunziata, G. Pugliano, and M. Migliaccio, “Reconstruction of the normalized radar cross section field from GNSS-R delay-Doppler map,” *IEEE J. Sel. Top. Appl. Earth Obs.*, vol. 7, no. 5, pp. 1573–1583, 2014.
- [56] L. Wang, G. Xie, and F. Qian, “Developing an innovative bimodal model to characterize the dynamic radar cross section of aircrafts,” *Digital Signal Process.*, vol. 116, p. 103105, 2021.
- [57] L. Wang, G. Xie, F. Qian, Y. Jin, and K. Gao, “A novel model for analyzing the statistical properties of targets’ RCS,” *IEEE Signal Process Lett.*, vol. 29, pp. 583–586, 2021.
- [58] Y.-Q. Zhuang, C.-X. Zhang, and X.-K. Zhang, “Dynamic RCS statistical characterization of aircraft target using Gaussian mixture density model (gmdm).”
- [59] M. Barbary and P. Zong, “Optimisation for stealth target detection based on stratospheric balloon-borne netted radar system,” *IET Radar, Sonar & Navigation*, vol. 9, no. 7, pp. 802–816, 2015.
- [60] A. Freundorfer, J. Siddiqui, and Y. Antar, “Radar cross-sectional study using noise radar,” in *Radar Sensor Technology XIX; and Active and Passive Signatures VI*, vol. 9461. SPIE, 2015, pp. 259–267.
- [61] B. H. Borden and M. L. Mumford, “A statistical glint/radar cross section target model,” *IEEE Trans. Aerosp. Electron. Syst.*, no. 5, pp. 781–785, 1983.
- [62] D. Wang, C. Zhang, and Y. Zhuang, “An analysis of the impact of movement feature on aircraft dynamic RCS statistical characteristics,” *J. Air Force Eng. Univ.(Natural Sci. Ed.)*, vol. 16, no. 4, pp. 19–23, 2015.
- [63] K. K. Talukdar and W. D. Lawing, “Estimation of the parameters of the rice distribution,” *the Journal of the Acoustical Society of America*, vol. 89, no. 3, pp. 1193–1197, 1991.
- [64] “RCS distribution fitting using improved nonparametric model,” in *2022 IEEE 10th Joint International Information Technology and Artificial Intelligence Conference (ITAIC)*, vol. 10. IEEE, 2022, pp. 350–354.
- [65] Y. Zhuang, C. Zhang, and X. Zhang, “A statistical analysis of radar targets’ RCS based on GMDM,” *J. Air Force Eng. Univ.: Natural Sci. Ed.*, vol. 15, no. 2, pp. 37–40, 2014.
- [66] E. F. Knott, J. F. Schaeffer, and M. T. Tully, *Radar cross section*. SciTech Publishing, 2004.
- [67] D. K. Barton, “Modern radar system analysis,” *Norwood*, 1988.
- [68] S. Haykin, R. Bakker, and B. W. Currie, “Uncovering nonlinear dynamics—the case study of sea clutter,” *Proc. IEEE*, vol. 90, no. 5, pp. 860–881, 2002.
- [69] Z. Xin, G. Liao, Z. Yang, Y. Zhang, and H. Dang, “A deterministic sea-clutter space-time model based on physical sea surface,” *IEEE Trans. Geosci. Remote Sens.*, vol. 54, no. 11, pp. 6659–6673, 2016.
- [70] R. A. Simon and P. V. Kumar, “A nonlinear sea clutter analysis using chaotic system,” in *2013 Fourth International Conference on Computing, Communications and Networking Technologies (ICCCNT)*. IEEE, 2013, pp. 1–5.
- [71] H. Liu, W. Xiong, and J. Song, “Analysis of sea clutter characteristics at high grazing angle,” in *2017 International Conference on Computer Systems, Electronics and Control (ICCSEC)*. IEEE, 2017, pp. 216–220.
- [72] V. Louf, A. Protat, R. A. Warren, S. M. Collis, D. B. Wolff, S. Raunyar, C. Jakob, and W. A. Petersen, “An integrated approach to weather radar calibration and monitoring using ground clutter and satellite comparisons,” *J. Atmos. Oceanic Technol.*, vol. 36, no. 1, pp. 17–39, 2019.
- [73] D. Kumlu and I. Erer, “Clutter removal techniques in ground penetrating radar for landmine detection: A survey,” in *Operations Research for Military Organizations*. IGI Global, 2019, pp. 375–399.
- [74] K. Zebiri and A. Mezache, “Radar CFAR detection for multiple-targets situations for Weibull and log-normal distributed clutter,” *Signal, Image Video Process.*, vol. 15, pp. 1671–1678, 2021.
- [75] X.-Y. Hou and N. Morinaga, “Detection performance in K-distributed and correlated rayleigh clutters,” *IEEE Trans. Aerosp. Electron. Syst.*, vol. 25, no. 5, pp. 634–642, 1989.
- [76] S. Sayama, “Detection of target and suppression of sea and weather clutter in stormy weather by Weibull/CFAR,” *IEEJ Trans. Electr. Electron. Eng.*, vol. 16, no. 2, pp. 180–187, 2021.
- [77] D. Kim, A. J. Park, U.-S. Suh, D. Goo, D. Kim, B. Yoon, W.-S. Ra, and S. Kim, “Accurate clutter synthesis for heterogeneous textures and dynamic radar environments,” *IEEE Trans. Aerosp. Electron. Syst.*, vol. 58, no. 4, pp. 3427–3445, 2022.
- [78] F. D. A. García, H. R. C. Mora, G. Fraidenraich, and J. C. S. Santos Filho, “Square-law detection of exponential targets in Weibull-distributed ground clutter,” *IEEE Geosci. Remote Sens. Lett.*, vol. 18, no. 11, pp. 1956–1960, 2020.
- [79] D. S. Medeiros, F. D. A. García, R. Machado, J. C. S. Santos Filho, and O. Saotome, “CA-CFAR performance in K-Distributed sea clutter with fully correlated texture,” *IEEE Geosci. Remote Sens. Lett.*, 2023.
- [80] J. Zhao, R. Jiang, X. Wang, and H. Gao, “Robust CFAR detection for multiple targets in K-distributed sea clutter based on machine learning,” *Symmetry*, vol. 11, no. 12, p. 1482, 2019.
- [81] S. Sayama and S. Ishii, “Suppression of log-normal distributed weather clutter observed by an S-band radar,” 2013.
- [82] A. Farina, F. Gini, M. Greco, and L. Verrazzani, “High resolution sea clutter data: statistical analysis of recorded live data,” *IEE Proceedings-Radar, Sonar and Navigation*, vol. 144, no. 3, pp. 121–130, 1997.
- [83] M. Sekine, S. Ohtani, T. Musha, T. Irabu, E. Kiuchi, T. Hagsawa, and Y. Tomita, “Weibull-distributed ground clutter,” *IEEE Trans. Aerosp. Electron. Syst.*, no. 4, pp. 596–598, 1981.
- [84] S. Sayama and H. Sekine, “Weibull, log-Weibull and K-distributed ground clutter modeling analyzed by AIC,” *IEEE Trans. Aerosp. Electron. Syst.*, vol. 37, no. 3, pp. 1108–1113, 2001.
- [85] X. Qin, S. Zhou, H. Zou, and G. Gao, “A CFAR detection algorithm for generalized gamma distributed background in high-resolution SAR images,” *IEEE Geosci. Remote Sens. Lett.*, vol. 10, no. 4, pp. 806–810, 2012.
- [86] G. Gao, K. Ouyang, Y. Luo, S. Liang, and S. Zhou, “Scheme of parameter estimation for generalized gamma distribution and its application to ship detection in SAR images,” *IEEE Geosci. Remote Sens. Lett.*, vol. 55, no. 3, pp. 1812–1832, 2016.
- [87] X. Qin, S. Zhou, H. Zou, and G. Gao, “Statistical modeling of sea clutter in high-resolution SAR images using generalized gamma distribution,” in *2012 International Conference on Computer Vision in Remote Sensing*. IEEE, 2012, pp. 306–310.
- [88] P. Huang, Z. Zou, X.-G. Xia, X. Liu, and G. Liao, “A statistical model based on modified generalized-K distribution for sea clutter,” *IEEE Geosci. Remote Sens. Lett.*, vol. 19, pp. 1–5, 2021.
- [89] R. Shuang-qiao, L. Yong-xiang, L. Xiang, and Z. Zhao-wen, “Parameters estimation for generalized K-distributed clutter model,” in *2006 CIE International Conference on Radar*. IEEE, 2006, pp. 1–4.
- [90] E. Ollila, D. E. Tyler, V. Koivunen, and H. V. Poor, “Compound-Gaussian clutter modeling with an inverse Gaussian texture distribution,” *IEEE Signal Process Lett.*, vol. 19, no. 12, pp. 876–879, 2012.
- [91] E. P. Blasch and M. Hensel, “Fusion of distributions for radar clutter modeling,” in *Int. Conf. on Info Fusion*, 2004.
- [92] V. Anastassopoulos and G. A. Lampropoulos, “A generalized compound model for radar clutter,” in *Proceedings of 1994 IEEE National Radar Conference*. IEEE, 1994, pp. 41–45.
- [93] W. Shi, X.-W. Shi, and L. Xu, “Radar cross section (rcs) statistical characterization using weibull distribution,” *Microwave and Optical Technology Letters*, vol. 55, no. 6, pp. 1355–1358, 2013.

- [94] R. Manavalan, "Review of synthetic aperture radar frequency, polarization, and incidence angle data for mapping the inundated regions," *Journal of Applied Remote Sensing*, vol. 12, no. 2, pp. 021 501–021 501, 2018.
- [95] S. Watts, "Radar detection prediction in sea clutter using the compound k-distribution model," in *IEE Proceedings F (Communications, Radar and Signal Processing)*, vol. 132, no. 7. IET, 1985, pp. 613–620.
- [96] J. Jao, "Amplitude distribution of composite terrain radar clutter and the κ -distribution," *IEEE Trans. Antennas Propag.*, vol. 32, no. 10, pp. 1049–1062, 1984.
- [97] H. Yanhui, L. Feng, Z. Baobao, and W. Shunjun, "Simulation of coherent correlation K-distribution sea clutter based on SIRP," in *2006 CIE International Conference on Radar*. IEEE, 2006, pp. 1–4.
- [98] J. Li and J. Wang, "Extended target detection based on generalized compound model in high resolution SAR images," in *Second International Conference on Space Information Technology*, vol. 6795. SPIE, 2007, pp. 657–662.
- [99] M. S. Greco and S. Watts, "Radar clutter modeling and analysis," in *Academic Press Library in Signal Processing*. Elsevier, 2014, vol. 2, pp. 513–594.
- [100] S. D. Liyanaarachchi, T. Riihonen, C. B. Barneto, and M. Valkama, "Optimized waveforms for 5G-6G communication with sensing: Theory, simulations and experiments," *IEEE Trans. Wireless Commun.*, vol. 20, no. 12, pp. 8301–8315, 2021.
- [101] H. Zhang, Y. Zhang, J. Cosmas, N. Jawad, W. Li, R. Muller, and T. Jiang, "mmWave indoor channel measurement campaign for 5G new radio indoor broadcasting," *IEEE Trans. Broadcast.*, vol. 68, no. 2, pp. 331–344, 2022.
- [102] L. Yu, Y. Zhang, J. Zhang, and Z. Yuan, "Implementation framework and validation of cluster-nuclei based channel model using environmental mapping for 6G communication systems," *IEEE Trans. Broadcast.*, vol. 19, no. 4, pp. 1–13, 2022.
- [103] Q. Tang, J. Li, L. Wang, Y. Jia, and G. Cui, "Multipath imaging for NLOS targets behind an L-shaped corner with single-channel UWB radar," *IEEE Sens. J.*, vol. 22, no. 2, pp. 1531–1540, 2021.
- [104] J. Wang, J. Zhang, Y. Zhang, T. Jiang, L. Yu, and G. Liu, "Empirical analysis of sensing channel characteristics and environment effects at 28 GHz," in *2022 IEEE Globecom Workshops (GC Wkshps)*. IEEE, 2022, pp. 1323–1328.
- [105] J. Zhang, J. Wang, Y. Zhang, Y. Liu, Z. Chai, G. Liu, and T. Jiang, "Integrated sensing and communication channel: Measurements, characteristics, and modeling," *IEEE Commun. Mag.*, 2023.
- [106] Y. Cui, Q. Zhang, Z. Feng, Q. Wen, Z. Wei, F. Liu, and P. Zhang, "Seeing is not always believing: ISAC-Assisted predictive beam tracking in multipath channels," *IEEE Wireless Communications Letters*, vol. 13, no. 1, pp. 14–18, 2024.
- [107] W. Jiang, Z. Wei, S. Yang, Z. Feng, and P. Zhang, "Cooperation based joint active and passive sensing with asynchronous transceivers for perceptive mobile networks," *arXiv preprint arXiv:2312.02163*, 2023.
- [108] W. Jiang, D. Ma, Z. Wei, Z. Feng, and P. Zhang, "ISAC-NET: model-driven deep learning for integrated passive sensing and communication," *arXiv preprint arXiv:2307.15074*, 2023.
- [109] B. Lu, Z. Wei, L. Wang, R. Zhang, and Z. Feng, "ISAC 4D imaging system based on 5G downlink Millimeter wave signal," *arXiv preprint arXiv:2310.06401*, 2023.
- [110] R. Zhang, C. Jiang, S. Wu, Q. Zhou, X. Jing, and J. Mu, "Wi-Fi sensing for joint gesture recognition and human identification from few samples in human-computer interaction," *IEEE J. Sel. Areas Commun.*, vol. 40, no. 7, pp. 2193–2205, 2022.
- [111] J. Yang, C.-K. Wen, X. Yang, J. Xu, T. Du, and S. Jin, "Multi-domain cooperative SLAM: the enabler for integrated sensing and communications," *IEEE Trans. Veh. Technol.*, vol. 30, no. 1, pp. 40–49, 2023.
- [112] Z. Wei, W. Jiang, Z. Feng, H. Wu, N. Zhang, K. Han, R. Xu, and P. Zhang, "Integrated sensing and communication enabled multiple base stations cooperative sensing towards 6G," *IEEE Network*, 2023.
- [113] C. Wang, Z. Wei, W. Jiang, H. Jiang, and Z. Feng, "Cooperative sensing enhanced UAV path-following and obstacle avoidance with variable formation," *IEEE Trans. Veh. Technol.*, pp. 1–16, 2024.
- [114] Z. Wei, W. Jiang, Z. Feng, H. Wu, N. Zhang, K. Han, R. Xu, and P. Zhang, "Integrated sensing and communication enabled multiple base stations cooperative sensing towards 6G," *IEEE Network*, pp. 1–1, 2023.
- [115] Z. Wei, R. Xu, Z. Feng, H. Wu, N. Zhang, W. Jiang, and X. Yang, "Symbol-level integrated sensing and communication enabled multiple base stations cooperative sensing," *IEEE Trans. Veh. Technol.*, vol. 73, no. 1, pp. 724–738, 2024.